Inorg. Chem. **2005**, *44*, 852–861

Uranyl Complexation in Fluorinated Acids (HF, HBF_4, HPF_6, HTf_2N): A Combined Experimental and Theoretical Study

Clotilde Gaillard,*,† Antoine El Azzi,† Isabelle Billard,† Hélène Bolvin,‡ and Christoph Hennig§

IReS, CNRS/IN2P3, and Université L. Pasteur, B.P. 28, 67037 Strasbourg Cedex 2, France, Laboratoire de Chimie Quantique, Institut Le Bel, 4 rue Blaise Pascal, 67000 Strasbourg, France, and Institute of Radiochemistry, Forschungszentrum Rossendorf, P.O. Box 510119, 01314 Dresden, Germany

Received July 20, 2004

The aim of this work is to characterize the complexation ability of F^-, BF_4^-, PF_6^-, and Tf_2N^- toward uranyl ions in aqueous solution. These anions were chosen as they represent the anionic part of the most studied room-temperature ionic liquids. Time-resolved emission spectroscopy and X-ray absorption spectroscopy were used to retrieve structural data on the complexes formed. The results obtained were compared with computational data. Tf_2N^- does not complex uranyl, even at high concentration. Other fluorinated acids form inner-sphere complexes with U(VI), in a monodentate fashion in the case of BF_4^- and PF_6^-.

1. Introduction

Actinides and lanthanides partitioning is achieved through processes based on solvent extraction from aqueous solutions. Although the nature of the organic phase differs from a process to another (for instance TBP/kerosene in PUREX or TBP + CMPO/dodecane in TRUEX), they all have in common the use of organic solvents emitting volatile organic compounds (VOCs), which represent important health and environmental issues. Moreover, extractant/solvent miscibility problems or third-phase formation encountered during the liquid−liquid extractions impel finding better systems. In this context, the use of room-temperature ionic liquids (RTILs) seems very promising.[1−3] However, the original nature of RTILs makes necessary an improved understanding of the fundamental aspects of solvation and complexation of metallic ions in these media. For instance, it is expected that the anionic part of RTILs plays a major role in the solvation and complexation of cationic species. The most common anions composing RTILs are BF_4^-, PF_6^-, $(CF_3SO_2)_2N^-$ (further noted as Tf_2N^-), and F^-, the latter being produced by decomposition of PF_6^- in the presence of water.[4] Nevertheless, few basic data are available on their complexing abilities, in particular toward actinides and lanthanides, and the structure of the complexes possibly formed is unclear.

To better understand this point by use of comparisons, we have carried out a study on the interaction between uranium(VI) (chosen as representative of actinides) and the HF, HBF_4, HPF_6, and HTf_2N acids in water. Solutions were made at very low pH, to avoid the competing effect of the hydrolysis of uranyl. We have coupled experimental techniques (TRES, EXAFS), which are known to be powerful tools and computational studies, to determine the local structure of uranyl complexes.[5−7]

2. Experimental Details and Data Analysis

2.1. Chemicals. All solutions were prepared with ultrapure water (Milli-Q plus, Millipore). All other reagents, of the best available quality, were used as received: $HClO_4$ (70% in H_2O, Aldrich); $H(CF_3SO_2)_2N$ (Aldrich); HPF_6 (60% in H_2O, Aldrich) declared to contain 10% F^-; HBF_4 (48% in H_2O, Aldrich), for which the

* Author to whom correspondence should be addressed. E-mail: cgaillar@ires.in2p3.fr.
† IReS, CNRS/IN2P3, and Université L. Pasteur.
‡ Institut Le Bel.
§ Forschungszentrum Rossendorf.

(1) Wasserscheid, P.; Welton, T. *Ionic Liquids in Synthesis*; Wiley-VCH: Weinheim, Germany, 2003.
(2) Huddleston, J. G.; Visser, A. E.; Reichert, W. M.; Willauer, H.; Broker, G.; Rogers, R. D. *Green Chem.* **2001**, *3*, 156.
(3) Visser, A. E.; Swatloski, R. P.; Reichert, W. M.; Mayton, R.; Sheff, S.; Wierzbicki, A.; Davis, J. H.; Rogers, R. D. *Environ. Sci. Technol.* **2002**, *36*, 2523.
(4) Swatloski, R. P.; Holbrey, J. D.; Rogers, R. D. *Green Chem.* **2003**, *5*, 361.
(5) Allen, P. G.; Shuh, D. K.; Bucher, J. J.; Edelstein, N. M.; Reich, T.; Denecke, M. A.; Nitsche, H. *Inorg. Chem.* **1996**, *35*, 784.
(6) Moll, H.; Denecke, M. A.; Jalilehvand, F.; Sandström, M.; Grenthe, I. *Inorg. Chem.* **1999**, *38*, 1795.
(7) Billard, I. In *Handbook on the physics and chemistry of rare earths*; Gschneider, K. A., Bünzli, J. C. G., Eds.; Elsevier: New York, 2003; Vol. 33.

10.1021/ic0490324 CCC: $30.25
Published on Web 01/25/2005

Table 1. EXAFS Structural Parameters of the Studied Complex[a]

sample	U(VI) speciation	shell	N	R (Å)	σ^2 (Å^2)	ΔE_0 (eV)	r factor
A (0.01 M UO_2^{2+}/1 M $HClO_4$)	100% $UO_2^{2+}{}_{aq}$	$U-O_{ax}$	2.0[b]	1.76	0.0018	−6.8	0.025
		$U-O_{eq}$	5.2	2.41	0.0066		
B (0.01 M UO_2^{2+}/3 M HTf_2N)	100% $UO_2^{2+}{}_{aq}$	$U-O_{ax}$	2.0[b]	1.76	0.0028	−6.8	0.012
		$U-O_{eq}$	4.4	2.41	0.0073		
C (0.01 M UO_2^{2+}/0.018 M NaF/1 M $HClO_4$	50% $UO_2^{2+}{}_{aq}$	1 eq-shell					
	50% UO_2F^+	$U-O_{ax}$	2.0[b]	1.77	0.0026	−6.4	0.015
		$U-O_{eq}$	3.2	2.42	0.0077		
		2 eq-shell					
		$U-O_{ax}$	2.0[b]	1.77	0.0028		
		U−F	0.5[b]	2.24	0.0048	−7.4	0.008
		$U-O_{eq}$	4.2	2.42	0.0087		
D (0.01 M UO_2^{2+}/1 M HBF_4)		1 eq-shell					
		$U-O_{ax}$	2.0[b]	1.77	0.0025	−6.3	0.014
		$U-O_{eq}$	4.5	2.41	0.0144		
		2 eq-shell					
		$U-O_{ax}$	2.0[b]	1.77	0.0029		
		U−F	1.0[c]	2.24	0.0068	−7.1	0.009
		$U-O_{eq}$	4.0[c]	2.44	0.0075		

[a] N is the coordination number, R the distance, σ^2 the Debye−Waller factor, ΔE_0 the threshold energy shift, and r factor the fit residual. [b] Fixed variable. [c] $N_F + N_O = 5$, $R \pm 0.02$ Å, and $N \pm 20\%$.

amount of decomposed F^- is not provided by the manufacturer; NaF (Prolabo). Uranium(VI) was introduced as $UO_2(ClO_4)_2 \cdot 7H_2O$ (homemade synthesized; for synthesis and purity see ref 8).

2.2. Time-Resolved Emission Spectroscopy (TRES). For all the solutions examined by TRES, the uranyl concentration was 10^{-6} M. The chemical conditions were the following:

(i) $[HClO_4] = 1$ M; (ii) HTf_2N series, 10^{-3} M $\leq [HTf_2N] \leq 1$ M, $[HClO_4] = 1$ M for $[HTf_2N] \leq 10^{-2}$ M, and $[HClO_4] = 0$ M for $[HTf_2N] > 10^{-2}$ M; (iii) HF/NaF series, 3.33×10^{-5} M $\leq$ $[NaF] \leq 10^{-3}$ M and $[HClO_4] = 1$ M; (iv) HBF_4 series, 5×10^{-5} M $\leq [HBF_4] \leq 1$ M and $[HClO_4] = 1.06$ M; (v) HPF_6 series, 10^{-6} M $\leq [HPF_6] \leq 10^{-2}$ M and $[HClO_4] = 1$ M.

All TRES experiments were performed with an excitation wavelength of 266 nm (Nd:YAG laser, 10 Hz, 6 ns pulse duration). The laser intensity is monitored with a powermeter (Scientech). The luminescence intensity as a function of time after excitation is selected via a monochromator and directed to a photomultiplier, connected to a fast oscilloscope. The laser setup is not corrected for light collection efficiency in the wavelength range investigated.

The experimental data are either decay spectra, acquired at a given wavelength, or emission spectra. For lifetime determinations, the decay spectra were recorded at a wavelength corresponding to the maximum of the emission spectra, either 488 or 494 nm, depending on the main species in solution (see below). The uncertainty on the lifetime values is on the order of ±3%. By integration of all counts acquired at a given wavelength, the raw luminescence intensity is obtained at this wavelength. These data, plotted as a function of the emission wavelength (in the range 480−580 nm), correspond to the raw emission spectrum of the sample. The precision of the monochromator is equal to ±0.25 nm and the resolution is of the order of ±0.3 nm, but the emission spectra were recorded with 1 nm steps. Depending on the amount of light emitted by the sample, either two or three maxima in the emission spectra could be resolved with confidence and are thus indicated. The luminescence ratio of two samples, ρ, is obtained by integrating the light collected in the whole emission range for each sample and normalizing the ratio value to the laser intensity. Repeated measurements (lifetimes and emission spectra) of some samples of the highest concentrations (HPF_6 and HBF_4 series) proved that the solutions were not altered by laser irradiation but an effect was observed for the NaF series (see below). No effect of the possible F^-/HF concentration was observed onto the quartz cuvette walls within the time required for the experiments, for any series of concern. All experiments were performed at $T = 298 \pm 1$ K.

Elaborate data analysis was performed both on lifetime and emission data. When two exponentials are present, a biexponential analysis of all the decay spectra recorded in the range 480−580 nm allows on to obtain the individual emission spectra of the two luminescent species present in solution, associated with lifetimes τ_1 and τ_2. By comparison with the raw emission spectrum of the sample, the individual relative intensities of both luminescent species can be calculated. Such a data analysis (individual spectra and associated intensities) will be called a decomposition in the following. In addition, chemometrics[9] was used to analyze the emission spectra, to derive the number of luminescent species present in the solution and their associated individual emission spectra. The program used for the principal component analysis (PCA) is based on that written by Pochon and co-workers,[10] which has been adapted to the emission spectra of this work (HBF_4 series).

2.3. EXAFS. 2.3.1. Sample Preparation. A description of the samples analyzed is given in Table 1, as well as the corresponding U(VI) speciation in solution when it is known. The uranium(VI) concentration was 0.01 M for all samples.

Attempts were made to characterize the UO_2^{2+} complex formed in HPF_6 solution (X_2). However, due to the low complexation constant, the uranyl concentration required to get only 35% of X_2 in a 3.2 M HPF_6 solution was too small (7×10^{-4} M) to get a reasonable signal.

2.3.2. Data Analysis. For the experiments, the samples were sealed in polyethylene containers. EXAFS experiments were carried out on the Rossendorf Beamline (ROBL) at the European Synchrotron Radiation Facility (ESRF). This beamline uses a Si(111) double crystal monochromator and two Pt mirrors for rejection of higher harmonics. The uranium L_{III} edge spectra were recorded at room temperature in transmission mode using argon flushed ionization chambers. The monochromator energy was calibrated against the first inflection point of the K-edge of Y metal (17038 eV).

(8) Bouby, M. Thesis, University L. Pasteur, Strasbourg, France, 1998 (in French).
(9) Malinowski, E. R. *Factor analysis in chemistry*, 2nd ed.; Wiley Interscience: New York, 1991.
(10) Pochon, P.; Moisy, P.; Donnet, L.; de Brauer, C.; Blanc, P. *Phys. Chem. Chem. Phys.* **2000**, *2*, 3813.

Data were analyzed using the EXAFS98 code,[11] according to standard procedures. Fourier transform to real space was made using k^3 weighting between 2.4 and 13.5 Å^{-1}, except for sample **A** (2.4−12.4 Å^{-1}). The phase and amplitude functions used to fit each set of data were calculated by FEFF8.1[12] from the crystal structure of uranyl perchlorate[13] $UO_2(ClO_4)_2 \cdot 7H_2O$ and uranyl difluoride UO_2F_2.[14] Fits were performed using Round Midnight code.[11] Fitting procedure were carried out in $k\chi(k)$ for the filtered back-transform EXAFS oscillations between 0.6 and 2.80 Å. The amplitude reduction factor S_0^2 was fixed to 1.0 for all fits. The shift in the threshold energy, ΔE_0, was allowed to vary as a global parameter for all atoms in each of the fits. Goodness of the fit was evaluated by the *r* factor.

2.4. Computational Details. All calculations have been performed with the energy-consistent relativistic effective core potentials (RECPs) suggested by the Stuttgart group.[15] For the uranium atom, the core consists of the 1s−4s, 2p−4p, 3d and 4d, and 4f atomic orbitals, and the basis set is [12s11p10d8f]/(8s7p6d4f). For boron, oxygen, and fluorine atoms, the 1s orbital is in the core, and the basis set is [4s4p]/(2s2p) for boron and is [4s5p2d]/(2s3p2d) for oxygen and fluorine. For the phosphorus atom, 1s and 2s orbitals are in the core and the basis set is [4s4p]/(2s2p). No g functions have been added on the uranium atom because they have only a very small influence on bond lengths in closed-shell systems. Basis sets are of double-ζ quality for boron and phosphorus that are positively charged and of triple-ζ plus polarization for oxygen and fluorine that are electronegative and directly involved in the intermolecular interactions.

All calculations have been performed with the Gaussian 98 program[16] at the DFT level using the hybrid functional B3LYP.[17−19] To describe solvation, we used the polarizable continuum model using the polarizable conductor calculation model CPCM[20] with parameters for water. All geometry optimizations have been done without symmetry constraints. Scalar relativistic effects are taken into account by the ECPs, but we have neglected spin−orbit effects. The latter are in general not important for the ground state of closed-shell systems and of minor importance for the structure of actinide complexes with an open f-shell.[21]

3. Results and Discussion

3.1. Time-Resolved Emission Spectroscopy. 3.1.1. $HClO_4$ Alone. For the sample solely containing uranyl and $HClO_4$ (1 M), both the uranyl lifetime ($\tau = 8.25$ μs) and the emission maximum wavelengths (487, 509, and 533 nm) are in good agreement with the values determined in an intercomparison experiment for UO_2^{2+} under the same chemical conditions.[22]

3.1.2. HTf_2N. HTf_2N is a strong acid and thus the effective concentration of Tf_2N^- in the solution equals that of the acid introduced so that we will refer to $[Tf_2N^-]$ in the following. Whatever $[Tf_2N^-]$, the decay spectra could be satisfactorily fitted with a monoexponential function, but the lifetime value depends on the solution composition. For $[Tf_2N^-] = 1$ M, the lifetime is equal to 3.5 μs. By contrast, the values of the maximum of the emission spectra are constant (see Table 2). The change in the lifetime as a function of $[Tf_2N^-]$, together with the absence of changes in the emission spectra, indicates that the Tf_2N^- anion does not complex uranyl, even for $[Tf_2N^-] = 1$ M, so that the luminescent species detected in the solutions is $UO_2^{2+}{}_{aq}$. This is in agreement with the poor complexing abilities of the Tf_2N^- anion in solution. The lifetime variations as a function of $[Tf_2N^-]$ are ascribed to long-range interactions. Such a phenomenon has already been observed in the case of ClO_4^-, and a detailed study has been performed on this subject.[23−26] Therefore, to fix the ionic strength of uranyl aqueous solutions, even up to high values, without complexation of the uranyl moiety, $HTf_2N/NaTf_2N$ can be safely used in replacement of $HClO_4$/$NaClO_4$, which oxidizing and explosive properties are not favorable in most cases.

3.1.3. NaF with $HClO_4$. Although NaF is fully dissociated in solution, the effective F^- concentration may not be equal to that of NaF introduced, owing to the presence of HF, a weak acid. Therefore, we will refer to $[F^-]_{tot}$ in the following. For $[F^-]_{tot} \leq 5 \times 10^{-4}$ M, the single lifetime observed is equal to $\tau = 8.4$ μs, while the first two emission peaks are located at 488 and 509 nm. According to a recent intercomparison test,[22] the lifetime and emission wavelength values observed in this work for $[F^-]_{tot} \leq 5 \times 10^{-4}$ M correspond to free $UO_2^{2+}{}_{aq}$ in 1 M $HClO_4$ and cannot be ascribed to any uranyl fluoro complex. The absence of complexation in this case is certainly due to the very high acidity of the solution, which limits the presence of F^-, owing to the strong association of HF.

Above $[F^-]_{tot} = 5 \times 10^{-4}$ M, a biexponential decay is obtained, and an effect of irradiation is observed, with the

(11) Michalowicz, A. *J. Phys. IV C2* **1997**, *7*, 235.
(12) Ankudinov, A.; Rehr, J. *Phys. Rev. B* **2000**, *62*, 2437.
(13) Alcock, N. W.; Esperas, S. *J. Chem. Soc., Dalton Trans.* **1977**, 893.
(14) Zachariasen, W. *Acta Crystallogr.* **1948**, *1*, 265.
(15) Küchle, W.; Dolg, M.; Stoll, H.; Preuss, H. *J. Chem. Phys.* **1994**, *100*, 7535.
(16) Frisch, M. J.; Trucks, G. W.; Schlegel, H. B.; Scuseria, G. E.; Robb, M. A.; Cheeseman, J. R.; Zakrzewski, V. G.; Montgomery, J. A.; Stratmann, R. E.; Burant, J. C.; Dapprich, S.; Millam, J. M.; Daniels, A. D.; Kudin, K. N.; Strain, M. C.; Farkas, O.; Tomasi, J.; Barone, V.; Cossi, M.; Cammi, R.; Mennucci, B.; Pomelli, C.; Adamo, C.; Clifford, S.; Ochterski, J.; Petersson, G. A.; Ayala, P. Y.; Cui, Q.; Morokuma, K.; Malick, D. K.; Rabuck, A. D.; Raghavachari, K.; Foresman, J. B.; Cioslowski, J.; Ortiz, J. V.; Stefanov, B. B.; Liu, G.; Liashenko, A.; Piskorz, P.; Komaromi, I.; Gomperts, R.; Martin, R. L.; Fox, D. J.; Keith, T.; Al-Laham, M. A.; Peng, C. Y.; Nanayakkara, A.; Gonzales, C.; Challacombe, M.; Gill, P. M. W.; Johnson, B. G.; Chen, W.; Wong, M. W.; Andres, J. L.; Head-Gordon, M.; Replonge, E. S.; Pople, J. A. *Gaussian 98*, revison A.9; Gaussian Inc.: Pittsburgh, PA, 1998.
(17) Becke, A. D. *Phys. Rev. A* **1988**, *38*, 3098.
(18) Lee, C.; Yang, W.; Parr, R. G. *Phys. Rev. B* **1988**, *37*, 785.
(19) Stevens, P. J.; Devlin, J. F.; Chabalowski, C. F.; Frisch, M. J. *J. Phys. Chem.* **1994**, *98*, 11623.
(20) Baronne, V.; Cossi, M.; Tomasi, J. *J. Comput. Chem.* **1998**, *19*, 404.
(21) Vallet, V.; Maron, L.; Schimmelpfennig, B.; Leininger, T.; Teichteil, C.; Gropen, O.; Grenthe, I.; Wahlgren, U. *J. Phys. Chem. A* **1999**, *103*, 9285.
(22) Billard, I.; Ansoborlo, E.; Apperson, K.; Arpigny, S.; Azenha, A. E.; Birch, D.; Bros, P.; Burrows, H.; Choppin, G. R.; Couston, L.; Dubois, V.; Fanghänel, T.; Geipel, G.; Hubert, S.; Kim, J. I.; Kimura, T.; Klenze, R.; Kronenberg, A.; Kumke, M.; Lagarde, G.; Lamarque, G.; Lis, S.; Madic, C.; Meinrath, G.; Moulin, C.; Nagaishi, R.; Parker, D.; Plancque, G.; Scherbaum, F.; Simoni, E.; Sinkov, S.; Viallesoubranne, C. *Appl. Spectrosc.* **2003**, *57*, 1027.
(23) Billard, I.; Rustenholtz, A.; Sémon, L.; Lützenkirchen, K. *Chem. Phys.* **2001**, *270*, 345.
(24) Bouby, M.; Billard, I.; Bonnenfant, A.; Klein, G. *Chem. Phys.* **1999**, *240*, 353.
(25) Rustenholtz, A.; Billard, I.; Duplâtre, G.; Lützenkirchen, K.; Sémon, L. *Radiochim. Acta* **2001**, *89*, 83.
(26) Sémon, L.; Boehme, C.; Billard, I.; Hennig, C.; Lützenkirchen, K.; Reich, T.; Rossberg, A.; Rossini, I.; Wipff, G. *Chem. Phys. Chem.* **2001**, *2*, 101.

Table 2. Spectroscopic Characteristics (Lifetime and Maximum Emission Wavelengths) of the Various Species Observed in This Work[a]

system	species	emission peaks (nm)	lifetime (μs)	K_{app} (M^{-1})	ref
UO_2^{2+}/$HClO_4$	$UO_2^{2+}{}_{aq}$	487.9 ± 0.8	7.9 ± 0.7		
		509.8 ± 0.6			22
		533.6 ± 0.6			
UO_2^{2+}/NaF(pH = 1.96; $I = 1.25 \times 10^{-2}$ M)	UO_2F^+	494 ± 1			
		515.5 ± 0.8	4.3 ± 0.2		22
		540 ± 2			
UO_2^{2+}/NaF	$UO_2^{2+}{}_{aq}$	488	8.4		this work
		509			
	UO_2F^+	nd	58		
UO_2^{2+}/HTf_2N	$UO_2^{2+}{}_{aq}$	487.0 ± 0.5	*b*		this work
		509.1 ± 0.2	*b*		
UO_2^{2+}/HBF_4	$UO_2^{2+}{}_{aq}$	487.5 ± 0.8	7.8 ± 0.3		
		509.7 ± 0.8			
		533.1 ± 0.6			this work
	X_1	493.5 ± 0.5			
		515.1 ± 0.5	40 ± 3	187	
		539.4 ± 0.8			
UO_2^{2+}/HPF_6	$UO_2^{2+}{}_{aq}$	488.0 ± 0.1			this work
		510.1 ± 0.6	8.1 ± 0.4		
		533 ± 1			
	X_2	493.4 ± 0.7			
		516.0 ± 0.3	46 ± 1		
		539.5 ± 0.5			

[a] See text. Uranyl complexes characterized in HBF_4 and HPF_6 solutions are noted respectively X_1 and X_2. Spectroscopic characteristics of $UO_2^{2+}{}_{aq}$ and UO_2F^+ as determined in ref 22. nd = not determined. [b] Lifetime depends on the [HTf_2N] value (see text).

two lifetimes increasing steadily with the irradiation duration. This has hampered any determination of the emission peaks. For a fresh solution, the longest lifetime, as derived from a single decay, is equal to 58 μs (relative intensity: 15%). The value $\tau_2 = 58$ μs derived in this work is close to that ascribed to UO_2F^+ in a previous publication[27] for roughly similar chemical conditions ($\tau_2 = 50$ μs, ionic strength equal to 1 M, by addition of $NaClO_4$). The difference with the lifetime of 4.3 μs observed for UO_2F^+ in the round-robin test is ascribed to the large difference in the ionic strength.[22]

Therefore, we conclude that fluoride complexation of UO_2^{2+} cannot be observed in our case for $[F^-]_{tot} \leq 5 \times 10^{-4}$ M and that the fluoride complex observed above this limit displays a lifetime equal to 58 μs.

3.1.4. HBF_4 and HPF_6. Similarly, we will refer to $[BF_4^-]_{tot}$ and $[PF_6^-]_{tot}$ (see below). By contrast with the HTf_2N series, the decay spectra for the HPF_6 and HBF_4 series could not be fitted with a monoexponential function, at any wavelength. A biexponential function appeared satisfactory but, for the limiting concentrations ($[BF_4^-]_{tot} = 5 \times 10^{-5}$ M or $[BF_4^-]_{tot} \geq 0.5$ M and $[PF_6^-]_{tot} \leq 5 \times 10^{-5}$ M), the biexponential analysis was tedious, owing to the low intensity of one of the lifetimes. Figure 1 presents the lifetime values obtained for a biexponential fit of the decay curves, as a function of $[X^-]_{tot}$ added. The shape of the emission spectra is affected by the amount of X^- added, as illustrated in Figures 2 and 3 for the HBF_4 and HPF_6 series, respectively.

For the HBF_4 series, the two lifetime values are constant for the whole $[BF_4^-]_{tot}$ range investigated, at $\tau_1 = 7.8 \pm 0.3$ μs and $\tau_2 = 40 \pm 3$ μs. Decompositions of the emission spectra were thus performed, leading to two individual emission spectra, associated with τ_1 and τ_2, which emission maximum (487.5 ± 0.8, 509.7 ± 0.8, 533.1 ± 0.6 nm for τ_1; 493.5 ± 0.5, 515.1 ± 0.5, 539.4 ± 0.8 nm for τ_2) are constant as a function of $[BF_4^-]_{tot}$. As an example, Figure 4 displays the total emission spectrum, together with the two individual spectra obtained by the decomposition procedure

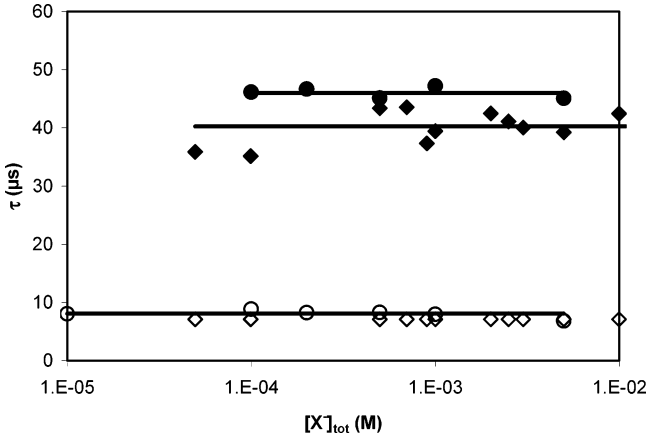

Figure 1. Lifetime values (τ_1, τ_2, μs) derived from a biexponential analysis of the decays: (●) τ_2, HPF_6 series; (○) τ_1, HPF_6 series; (◆) τ_2, HBF_4 series; (◇) τ_1, HBF_4 series. Solid lines are the average values.

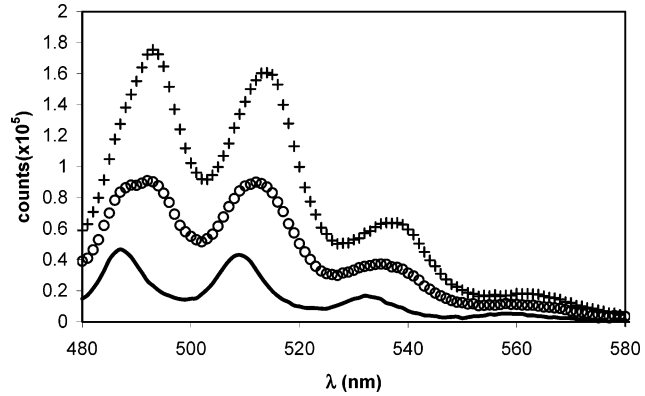

Figure 2. Emission spectra as a function of $[BF_4^-]_{tot}$: solid line, $[BF_4^-]_{tot} = 0$ M; dots, $[BF_4^-]_{tot} = 1.5 \times 10^{-3}$ M; crosses, $[BF_4^-]_{tot} = 0.03$ M.

(27) Fazekas, Z.; Yamamura, T.; Tomiyasu, H. *J. Alloys Compd.* **1998**, *271/273*, 756.

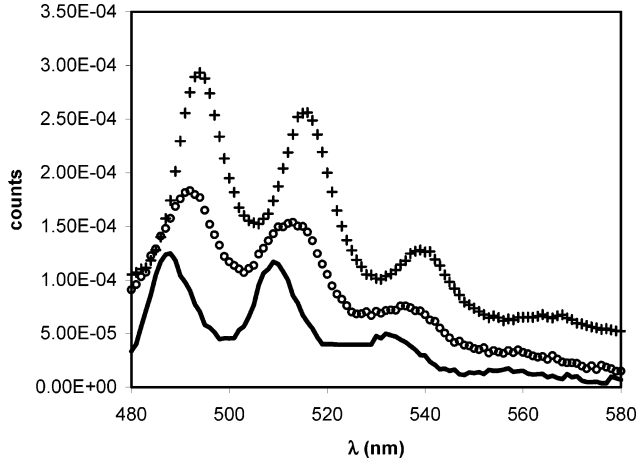

Figure 3. Emission spectra as a function of $[PF_6^-]_{tot}$ concentration: solid line, $[PF_6^-]_{tot} = 10^{-4}$ M; dots, $[PF_6^-]_{tot} = 10^{-3}$ M; crosses, $[PF_6^-]_{tot} = 10^{-2}$ M.

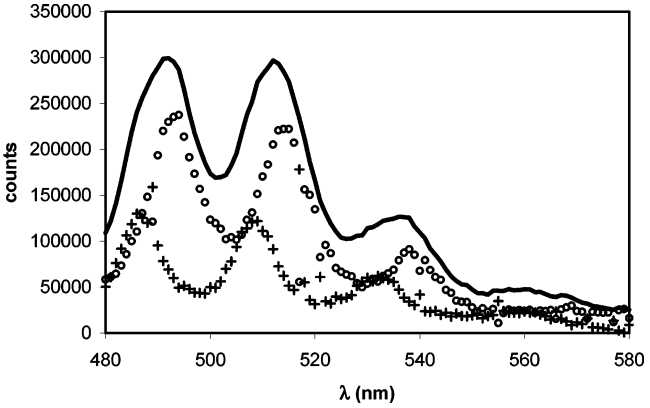

Figure 4. Decomposition of the emission spectrum obtained for $[HBF_4] = 2.5 \times 10^{-3}$ M: solid line, total emission spectrum; +, individual intensity, I_1, associated with τ_1; ○, individual intensity, I_2, associated with τ_2.

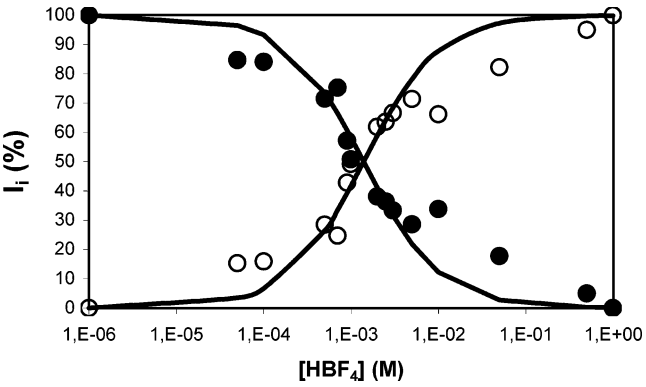

Figure 5. Individual intensities, I_1 and I_2, as a function of HBF_4 concentration: symbols, experimental data; solid lines, best fit (see text).

for $[BF_4^-]_{tot} = 2.5 \times 10^{-3}$ M. Figure 5 presents the intensities associated with τ_1 and τ_2 as a function of $[BF_4^-]_{tot}$ added. The PCA analysis confirms that two independent species are present in solution. The peaks of the corresponding two emission spectra are calculated at 488, 510, and 534 nm (first species) and 493, 516, and 539 nm (second species). These values agree very well with the values obtained from the decomposition procedure. Finally, the luminescence ratio of the complex to UO_2^{2+} is equal to 5 and is obtained by dividing the luminescence intensity of the sample containing $[BF_4^-]_{tot} = 1$ M to that with no BF_4^-.

Similarly, for the HPF_6 series, the two lifetimes ($\tau_1 = 8.1 \pm 0.4$ μs and $\tau_2 = 46 \pm 1$ μs) are constant as a function of $[PF_6^-]_{tot}$ added up to 5×10^{-3} M. Above this concentration, the τ_2 lifetime is equal to 73 μs, but in this case, a fit with a triexponential function did not appear convincing. Decompositions of the emission spectra were thus performed for all samples with $[PF_6^-]_{tot} \leq 5 \times 10^{-3}$ M, to give two individual emission spectra which maximum emission wavelengths are constant as a function of $[PF_6^-]_{tot}$. Table 2 summarizes the spectroscopic characteristics (emission maximum and lifetimes) of the species observed in this work, together with published data for the ease of comparison. Owing to the presence of an additional lifetime equal to 73 μs at high $[PF_6^-]_{tot}$ values, the luminescence ratio was not determined.

For both series, the red shift observed in the emission spectra (see Figures 2 and 3) as the $[X^-]_{tot}$ value is increased is the signature of a complexation process. The complexation process is further assessed by the existence of a biexponential decay (see Figure 1). For the HBF_4 series, the two lifetimes τ_1 and τ_2 are constant as a function of the ligand concentration, implying that a single complexation reaction occurs in the ground state, with no photochemical equivalent in the excited state.[28,29] Furthermore, it implies that the luminescent complex is the same in the whole range investigated. Similar conclusions can be derived for the HPF_6 series, up to 5×10^{-3} M. The sudden change in τ_2 at the highest HPF_6 concentrations investigated in this study is most probably due to the appearance of another complexing moieties, which competes successfully with the one observed below 5×10^{-3} M, or to the formation of a 1:2 complex.

By a comparison of our decomposition results (HBF_4 and HPF_6 series; see Table 2) with the values of the round-robin test performed for U(VI) aqueous solutions,[22] it is clear that, for both series, the species displaying the shortest lifetime is $UO_2^{2+}{}_{aq}$, so that the lifetime τ_2 can be ascribed to the complex formed. To tentatively ascribe a chemical formula to the complexes observed, the speciation should be known. Though HBF_4 and HPF_6 are strong acids, the exact chemical composition of the solutions is difficult to estimate, due to the possible decomposition of both BF_4^- and PF_6^- anions (to give BF_3 and F^-, $K = 10^{2.3}$,[30] or PF_5 and F^-, equilibrium constant not documented) and the subsequent weak acid equilibrium of HF ($pK_a = 3.14$).[30] Due to the low pH value, mostly driven by the $HClO_4$ concentration (equal to 1 M for all samples; see section 2.2), it can be hypothesised that the $[F^-]_{tot}$ value is too low for complexation with uranyl. This assumption is confirmed by comparing the NaF, HBF_4, and HPF_6 series: while no complexation is observed for the NaF series up to $[F^-]_{tot} = 5 \times 10^{-4}$ M, complexation is already significant for the HBF_4 and HPF_6 series for $[X^-]_{tot} = 5 \times 10^{-4}$ M. A biexponential decay is clearly observed, with a long lifetime displaying a relative intensity equal to ca. 25%

(28) Billard, I.; Lützenkirchen, K. *Radiochim. Acta* **2003**, *91*, 285.
(29) Horrocks, W. deW., Jr.; Arkle, V. K.; Liotta, F. J.; Sudnick, D. R. *J. Am. Chem. Soc.* **1983**, *105*, 3455.
(30) Sillen, L. G.; Martell, A. E. *Stability constants of metal-ion complexes*; The Chemical Society: London, 1964.

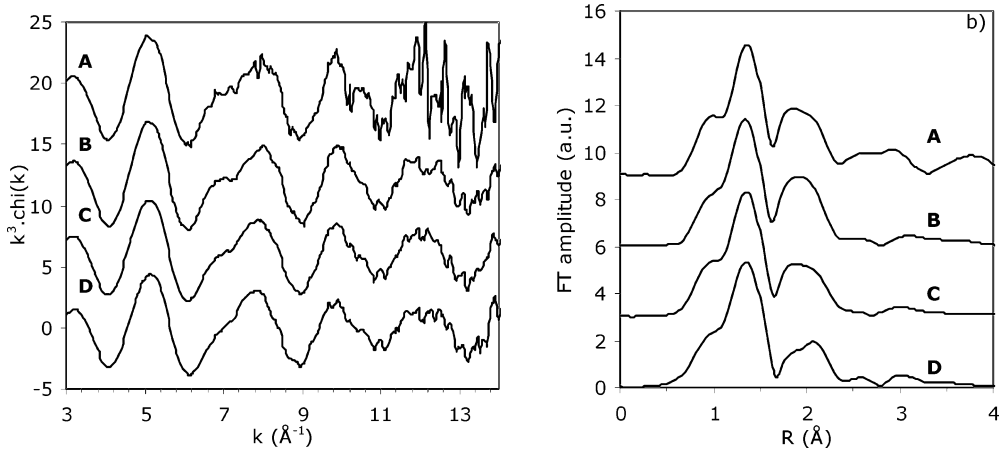

Figure 6. (a) Experimental EXAFS oscillations of samples **A**−**D**. For clarity, spectra were shifted along the ordinate axis. (b) Corresponding FT moduli (not phase corrected), shifted along ordinate axis for clarity.

in both cases and a τ_2 value significantly different from that observed in the NaF series (see Table 2). This shows that the complexation with F^- anions in the HBF_4 and HPF_6 series can be safely ruled out. Considering the values of the BF_4^-/BF_3 equilibrium, raw calculations show that whatever the initial concentration of HX, BF_3 is dominating the speciation. However, this does not mean that BF_3 is the complexing moieties: it is known to be a strong Lewis acid, so that it should not have any affinity toward metallic cations such as uranyl. Moreover, the complexing affinity of BF_4^- toward uranyl could be larger, owing to its negative charge. Furthermore, even very low amounts of uranyl complexes can be detected by TRES, provided that the luminescence quantum yield is large. This property, which is the basis of uranium assays by use of the strong complexing agent Flurane,[31] is also known for uranyl-hydrolyzed species[22,32] but is not documented for the ligands of this study. Therefore, although no precise information on the chemical formula of the complexes observed can be obtained by TRES, it can be reasonably hypothesised that the complexing moiety is BF_4^-.

Interestingly, the average τ_2 value for the HBF_4 series differs significantly from that of the HPF_6 and NaF series (see Table 2), while the wavelength maxima are very close for both series and match those obtained for UO_2F^+ in a previous publication.[22] By contrast with what is commonly observed, those complexes thus cannot be recognized with the help of their emission spectra nor can their lifetime values be a signature as the lifetime probably depends on the total ionic strength.[24] The maximum emission wavelengths are related to the vibrations of the complex. It is therefore possible that all three complexes display similar emission maximum, as all three ligands are bound to the uranyl moieties through the F atom.

In both HBF_4 and HPF_6 series, the emission shift upon complexation is equal to ca. 5 nm, which is an ideal case for the determination of the complexation constant by TRES.[22] In principle, owing to the biexponential nature of the decay spectra, the equilibrium constant can be derived without approximation from the plot of the individual intensities as a function of [L], the total ligand concentration.[28] However, in our case, various experimental reasons hamper the determination of the exact equilibrium constant and just an *apparent* equilibrium constant can be derived: (i) The total intensities are not corrected for the light collection efficiency. (ii) The ionic strength is high and is not constant. (iii) The exact concentration of the ligand is not known. In addition, for the HPF_6 series, the exact luminescence ratio is difficult to estimate as it was not possible to observe the complex displaying $\tau_2 = 46\ \mu$s alone in solution (see section 4). Therefore, only the apparent equilibrium constant was derived from the fit of the experimental HBF_4 data, assuming that the ligand concentration is equal to the total HBF_4 concentration. Solid lines in Figure 5 represent the best fit to the data, and the value of K is reported in Table 2. The variation in the ionic strength (above $[BF_4^-]_{tot} = 0.01$ M) is probably the reason for the discrepancy observed between the theoretical and the experimental curves.

3.2. EXAFS. Figure 6 displays the raw EXAFS spectra and the corresponding Fourier transforms for all samples. The structural parameters obtained are presented in Table 1, and best fits of the filtered EXAFS oscillations and the corresponding FT are presented in Figure 7. The FT peaks are shifted around $\Delta = 0.3-0.5$ Å to lower R values as a result of the phase shift of the photoelectron wave. Compared to $UO_2^{2+}{}_{aq}$ (**A**), slight differences are observed on the EXAFS oscillations between 6 and 9 $Å^{-1}$ for samples **C** and **D**. The axial oxygen atoms (O_{ax}) are not influenced by the ligands as indicated by the identical peak heights in the FT's. Otherwise a modification of the equatorial shell upon complexation is obvious on the Fourier transforms. Indeed, the shape of the peak centered at $R + \Delta = 2$ Å is strongly influenced by the complexation with fluorinated ligands. As a result the equatorial shell is broadened. Only a very weak broadening of the FT peak is noticed between sample **A** ($UO_2^{2+}{}_{aq}$) and sample **B** (UO_2^{2+}/HTf_2N).

3.2.1. $UO_2^{2+}{}_{aq}$ and UO_2^{2+}/HTf_2N. Structural data obtained for sample **A** agree well with the data previously reported

(31) Moulin, C.; Beaucaire, C.; Decambox, P.; Mauchien, P. *Anal. Chim. Acta* **1990**, *238*, 291.
(32) Moulin, C.; Laszak, I.; Moulin, V.; Tondre, C. *Appl. Spectrosc.* **1998**, *52*, 528.

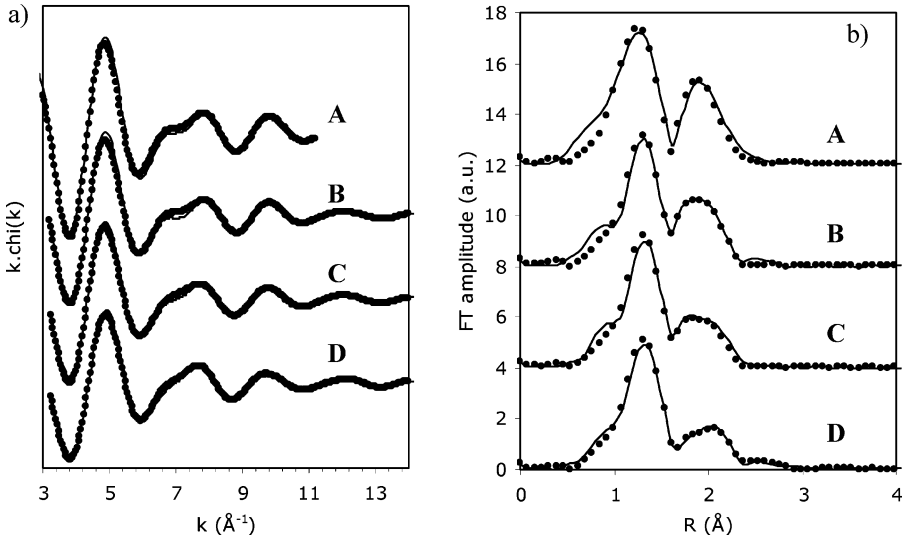

Figure 7. (a) Fitted (···) filtered EXAFS oscillations of samples **A**−**D**. For clarity, spectra were shifted along the ordinate axis. (b) Corresponding fitted (···) FT moduli, also shifted along the ordinate axis for clarity.

in the literature.[33] Only a very weak broadening of the FT peak can be obtained in sample **B**. Attempts to use a fit model with two equatorial shells for this sample did not lead to a coherent fit. The weak broadening is related with a small increase in the Debye−Waller factor, indicating that the coordination of uranium is nearly identical with the one of $UO_2^{2+}{}_{aq}$. There occurs no significant complexation between the uranyl ion and the Tf_2N^- anion.

3.2.2. UO_2^{2+}/NaF. For sample **C**, fits were made using models with one (O_{eq}) or two (O_{eq} and F) equatorial shells. In the latter case, the number of F neighbors was fixed to the value calculated from the U(VI) speciation in solution, to avoid correlation problems. Regarding the fit residual *r*, there is an improvement of the fit by including a fluorine shell. Moreover, when using exclusively one equatorial shell, the number of oxygens ($N_O = 3.2 \pm 0.6$) is not consistent with the average equatorial coordination number of uranyl of 5, which is typically related with a bond length of 2.42 Å. Thus, this model is highly unlikely. A two shells model comprising one oxygen and one fluorine shell results in a coherent equatorial coordination number ($N_{eq} = 4.7 \pm 0.8$), a U−O bond length of 2.42 ± 0.02 Å and a U−F bond length of 2.24 ± 0.02 Å. This U−F distance is commonly found in uranyl fluoride solid compounds[34,35] and was also characterized in fluoro complexes of uranium(VI) oxalate.[36] To our knowledge, only one experimental characterization of the UO_2^{2+}/F^- aqueous complexes was made using EXAFS by Vallet et al.[37] They have determined the structure of the 1:3, 1:4, and 1:5 complexes (namely $UO_2F_3^-$, $UO_2F_4^{2-}$, and $UO_2F_5^{3-}$). For the three species, U−F bond lengths were found in the range 2.25−2.26 Å, i.e., similar to the one measured in this work for the 1:1 complex. Vallet et al. did not measure any dependence of the number of fluoride ligands on the U−F bond length. This observation is confirmed by our study.

3.2.3. UO_2^{2+}/HBF_4. Fit results for sample **D** are also displayed in Table 1. HBF_4 decomposition in water leads to the formation of potentially two complexing species, BF_3 and BF_4^- (due to the low pH value, F^- are associated as HF). As explained in section 3.1.4, BF_3 complexation with uranyl ions is implausible, even if it constitutes the major species in solution. We can thus reasonably assume that the complex X_1 characterized in this study is $UO_2BF_4^+$.

If the data analysis is performed only with one equatorial shell of oxygen atoms, the fit result shows an anomalous large Debye−Waller factor. As a matter of fact, the fit is improved by including a fluorine shell. For this sample, contrary to **C**, the uranyl speciation in solution is not known (i.e. the ratio $X_1/UO_2^{2+}{}_{aq}$), which means that the number of fluorine atoms in the equatorial shell must be kept as a free parameter. To that purpose, we have assumed that the total equatorial number ($N_F + N_O$) is equal to 5. The result ($N_F = 1.0 \pm 0.2$) indicates either a total monodentate complexation of uranyl as X_1 or a mix between $UO_2^{2+}{}_{aq}$ and a bidentate complex. Nevertheless, the boron atom could not be detected due to its low backscattering amplitude. The U−F bond length is found identical with that in UO_2F^+ complex. To our knowledge, no data are available on the UO_2^{2+}/BF_4^- complexes in the literature. In a comparison with the trends observed for known systems such as uranyl−carbonate complexes,[38] a bidentate coordination would probably have increased the U−F distance. Similarly, the U−F bond length of U(VI) dimers has been determined to 2.33−2.37 Å.[39]

(33) Allen, P. G.; Bucher, J. J.; Shuh, D. K.; Edelstein, N. M.; Reich, T. *Inorg. Chem.* **1997**, *36*, 4676.
(34) Mak, T.; Yip, W. *Inorg. Chim. Acta* **1985**, *109*, 131.
(35) Nguyen, Q.; Chourou, S.; Heckly, J. *J. Inorg. Nucl. Chem.* **1981**, *43*, 1835.
(36) Vallet, V.; Moll, H.; Wahlgren, U.; Szabo, Z.; Grenthe, I. *Inorg. Chem.* **2003**, *42*, 1982.
(37) Vallet, V.; Wahlgren, U.; Schimmelpfennig, B.; Moll, H.; Szabo, Z.; Grenthe, I. *Inorg. Chem.* **2001**, *40*, 3516.
(38) Denecke, M.; Reich, T.; Bubner, M.; Pompe, S.; Heise, K.; Nitsche, H.; Allen, P.; Bucher, J.; Edelstein, N.; Shuh, D. *J. Alloys. Compd.* **1998**, *271/273*, 123.
(39) Walker, S. M.; Halasyamani, P. S.; Allen, S.; O'Hare, D. *J. Am. Chem. Soc.* **1999**, *121*, 10513.

Therefore, the short U−F bond length (2.24 Å) found for the $UO_2BF_4^+$ complex confirms the monodentate coordination.

We can notice that the structural data obtained for UO_2F^+ and $UO_2BF_4^+$ complexes are identical: same U−F bond lengths and for $UO_2BF_4^+$ the monodentate coordination implies a too long U−B distance to allow the detection of the boron atoms in the third shell. Thus, like TRES experiments, EXAFS could not give additional information to differentiate between F^- and BF_4^- complexes.

3.3. Computational Studies. The aim of this study is to compare different complexes. We have chosen to focus on the chemical variations from one system to another as gauged by a single method, namely B3LYP geometry optimizations of the molecule embedded in polarizable medium. This method has been chosen because it gave excellent results compared to EXAFS for oxo complexes of neptunium.[40] The uranyl ion is described with its first solvation sphere, and the further effect of solvation is taken into account by means of the polarization model. The interaction between uranyl and F^- has been studied already with similar methods. Wang et al.[41] have studied the UO_2F_2 complex with *n* water molecules using LDA and without any modeling for the solvent. They found U−F = 2.04 Å for *n* = 0, 2.12 Å for *n* = 3, and 2.31 Å for *n* = 4. It shows the influence of the number of water molecules in the first coordination sphere on the U−F distance and, in this case, that the coordination with six molecules in the equatorial plane is possible, even without continuum modeling the solvent. Vallet et al.[37] studied $[UO_2F_3(H_2O)_2]^-$, $[UO_2F_4(H_2O)]^{2-}$, and $[UO_2F_5]^{3-}$ in their different conformations. They used HF with CPCM modeling for the solvent. The U−F distance is 2.24 Å in the first complex, 2.25 Å in the second one, and 2.29 Å in the last one. Finally, Infante et al.[42] studied the effect of the solvation on the $[UO_2F_4]^{2-}$ complex comparing results from QM (quantum mechanics) and QM/MM (hybrid of QM and molecular mechanics methods) calculations. They show that the solvent must be described at least with the second shell to favor the coordination with five molecules in the equatorial plane compared to the coordination with four molecules in this plane and one obtains convergence of the results in terms of the description of different shells of solvation around the uranyl when at least the first shell of solvation is described by QM methods.

With the exception of one case, the first solvation sphere consists of five molecules. Complex **1** consists of uranyl with five water molecules, complexes **2**−**4** consist of uranyl surrounded by four water molecules and an anion, F^-, BF_4^-, or PF_6^-, respectively. As it will be discussed later on, the calculated U−F distances do not match the experimental ones; thus, other hypothesis have been tested. The influence of the second shell of solvation has been first modelized by adding a water molecule next to the F^-, forming complex **2′**. More molecules have been added around F^-, but the convergence was very low and it did not seem to have any effect on the U−F distance. Wang et al.[41] found a complex with six molecules in the equatorial plane: we checked this hypothesis with complex **2″** formed by **2′** plus one water molecule in the first solvation shell. In the case of uranyl plus BF_4^- different hypothesis have been tested too. First was tested the case where BF_4^- is linked with two fluorines to uranium forming complex **3′**, which is only surrounded by three water molecules. Finally, complex **3″** consists of uranyl and neutral BF_3 surrounded by four water molecules. Results are summarized in Table 3, and complexes **2′**, **3**, and **4** in their optimized geometry are shown in Figure 8. Both BF_4^- and PF_6^- form a hydrogen bond with a water molecule forming a six-membered ring with uranyl.

One can characterize the strength of the interaction between the anion and uranyl by the bond length U−F and by the charge donation to the uranyl, i.e., the Mulliken charge of the UO_2 unit. Even if the Mulliken charges are not an absolute criterion to analyze the charges of the fragments, they give good tendencies as long as same quality of basis sets and similar methods are used. The strongest interaction is with F^- anion, the most electronegative one, that gives 0.26 electron more than water to uranyl. BF_4^- shows an interaction slightly stronger than water giving 0.03 electron more than water while PF_6^- seems to have the same strength of interaction with uranyl as water. The bond lengths in uranyl, $U-O_{ax}$, compare very well with the experimental ones, and the $U-O_{eq}$ distances are in good agreement except for complexes **3**. These results are however quite different from the experimental ones when one considers the uranium−anion distance. EXAFS gives a U−F distance of 2.24 Å for

Table 3. Geometrical Characteristics of the Optimized Geometries of the Complexes $[UO_2^{2+} + 4H_2O + X]$ with Different Ligands X[a]

		geometry				Mulliken charges			
	system X	$U-O_{ax}$	OUO	U−X	$U-O_{eq}$	U	UO_2	X	H_2O
1	H_2O	1.76	180		2.45	2.29	1.09		0.18
2	F^-	1.78	175	2.13	2.50	2.13	0.83	−0.49	0.16
2′	$F^-\cdots H_2O$	1.78	175	2.16	2.50	2.14	0.84	−0.40	0.16
2″	$F^-\cdots H_2O + H_2O$	1.78	177	2.19	2.61	2.18	0.92	−0.63	0.14
3	BF_4^-	1.76	176	2.39	2.45	2.23	1.06	−0.79	0.18
3′	BF_4^- bidentate	1.76	176	2.46	2.40	2.23	1.11	−0.64	0.17
3″	BF_3	1.75	175	2.66	2.48	2.28	1.12	0.09	0.20
4	PF_6^-	1.76	176	2.40	2.45	2.30	1.10	−0.85	0.18

[a] $U-O_{ax}$ and OUO are the internal bond length and angle in the uranyl, U−X is the length between the uranium atom and the nearest atom of the X group, and $U-O_{eq}$ is the mean distance between uranium and the nearest atom of the surrounding water molecules. Distances are in Å, and angles are in deg. Mulliken charges are of the uranium atom, uranyl ion, X group, and (mean value) the water molecules in the optimized geometry.

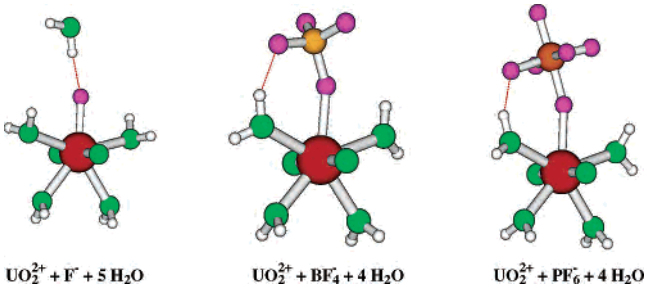

Figure 8. Complexes **2′**, **3**, and **4** (left to right) in their optimized geometry.

(40) Bolvin, H.; Wahlgren, U.; Moll, H.; Reich, T.; Geipel, G.; Fanghänel, T.; Grenthe, I. *J. Phys. Chem. A* **2001**, *105*, 11441.
(41) Wang, Q.; Pitzer, R. M. *J. Phys. Chem. A* **2001**, *105*, 8370.
(42) Infante, I.; Visscher, L. *Comput. Chem.* **2004**, *25*, 386.

Table 4. Geometrical Characteristics of the Optimized Geometries of the Complexes $[UO_2F_n(H_2O)_{5-n}]^{2-n}$ [a]

	geometry			Mulliken charges				
n	UO_{ax}	UF	UO_{eq}	U	UO_2	F	H_2O	Δq
0	1.76		2.45	2.29	1.09		0.18	
1	1.78	2.13	2.50	2.13	0.83	−0.49	0.16	0.24
2	1.79	2.17	2.55	2.06	0.76	−0.58	0.13	0.16
3	1.81	2.20	2.61	1.99	0.61	−0.62	0.12	0.15
4	1.83	2.25	2.56	1.97	0.51	−0.66	0.12	0.14
5	1.83	2.27		1.92	0.45	−0.69		0.13

[a] For the definitions and units, see Table 3. All numbers are averages on the different atoms of the same nature and on the different conformations of the complex when necessary. Δq is the excess charge/F^- given to UO_2^{2+} compared to water.

both F^- and BF_4^-, as found in sections 3.2.2 and 3.2.3, while modelization gives 2.13 and 2.39 Å, respectively. The bond length is much too short in one case and much too long in the other one, and they are very different while they are the same in the experimental case. The effect of the second solvation sphere has been checked through the study of complex **2′**: the U−F length becomes 0.03 Å longer when adding a water molecule around the F^- anion, forming an hydrogen bond. This water molecule takes some negative charge of the F^-, and the interaction with uranyl is reduced. Infante et al.[42] showed that the addition of second and third solvation shells by the mean of a QM/MM study did not have dramatic effects on the coordination in the first solvation sphere. We checked the hypothesis that the coordination number in the equatorial plane could be 6 by adding one water molecule in the coordination sphere: this cluster with six molecules in the equatorial plane of uranyl was not stable without solvent model, the extra molecule being expulsed to the second coordination sphere, but was stable with the solvent model. In this case, the U−F length is longer by 0.03 Å but the water molecules of the first sphere are even further away from uranyl and do not match the experimental values at all. For complexes **3**, some hypotheses have been checked: the bidentate one (complex **3′**) gives rise to a much longer U−F distance and the neutral BF_3 a distance even longer. Results for PF_6^- are in agreement with experiment (section 2.3): interaction of uranyl with water and PF_6^- seems to be of the same order of magnitude, which may explain why it is not detected in the coordination sphere of uranyl. To better analyze the coordination of fluoride anion, the whole series $[UO_2F_n(H_2O)_{5-n}]^{2-n}$, $n = 0-5$, has been studied; results are summarized in Table 4. Results are averaged on the different positions of a given atom and on the different conformers. It appears clearly that there is a cooperative effect that the bond is stronger with one anion and becomes weaker and weaker adding more anions. The whole charge of uranyl decreases, but the charge donation per F^- decreases. The length $U-O_{eq}$ tends to be larger when the Mulliken charge of uranyl decreases; thus, the larger is the number of anions or the strength of their charge donation, the longer is the distance to water molecules. For $n = 3-5$, one finds results coherent with the ones of Vallet and fitting well experimental values.

In conclusion, EXAFS gives a U−F distance almost independent of the number of F^- anions and of the nature of the anion, at least for F^- and BF_4^-, while calculation show a large cooperativity in the first solvation and a dependency of the nature of the anion. Results of calculations are rational: the distance of one molecule to uranyl depends strongly on the number and the nature of the other molecules in this sphere; an anion is more electrodonor than water is, so uranyl is less attractive for the next one. It seems logical that the strong electron-donor fluoride interacts more strongly with uranyl than BF_4^-, where the negative charge is much more diffuse. Calculations match well experimental results when there are four or five F^- anions in the coordination sphere, but the discrepancy is large when there is only one fluoride or one BF_4^-. In the first case, the distance is too small, which means that the electron donation of the other molecules, namely the water molecules, is underestimated. One can give two reasons to this discrepancy, a chemical one and a methodological one. The first reason could be the presence of other anions instead of water molecules that give more negative charge to uranyl and enlarge the U−F distance. As an example, we have studied the clusters $[UO_2F(H_2O)_{4-n}(OH^-)_n]^{2-n}$ and found a U−F distance of 2.13, 2.16, 2.25, 2.32, and 2.38 Å for $n = 0-4$. As previously in this work, distances are an average on the different conformers. This shows that the presence of another anion could be a reason for the large distance between U and F. But, in our case, the pH is very low so there are no hydroxide molecules in solution. Perchlorate anions ClO_4^- are also present in solution, but they have already been shown to be inert with uranyl.[25] The second reason could be the wrong description of water molecules that do not interact enough with uranyl. This could explain both the too long distance between water and uranyl and the too small distance with F^-. But these hypotheses do not explain the too long bond with BF_4^-.

4. Conclusions

We have combined experimental (TRES, EXAFS) and computational studies to grab information on the structure of the complexes formed in acidic water between uranyl and fluorinated inorganic ligands: F^-, BF_4^-, PF_6^-, Tf_2N^-. As explained in the introduction of this paper, these ligands constitute the anionic part of the most studied RTILs ($BumimPF_6$, $BumimBF_4$, and $BumimTf_2N$) and these experiments should therefore be of importance as references for complexation and solvation processes of cationic species in RTILs. Our experimental and theoretical results evidence large differences in the ability of these anions to interact with uranyl in aqueous solution. Tf_2N^- does not complex to uranyl, even at high concentrations. This means that water is to be considered as a strong complexing moiety in the solvation sphere in $BumimTf_2N$. Besides, TRES experiments showed how the europium coordination sphere was sensitive to a small amount of water in $BumimTf_2N$.[43]

The analysis of Mulliken charges shows that PF_6^- ions interact with uranyl with a quite similar strength compared

(43) Billard, I.; Mekki, S.; Gaillard, C.; Hesemann, P.; Moutiers, G.; Mariet, C.; Labet, A.; Bünzli, J. C. G. *Eur. J. Inorg. Chem.* **2004**, 1190.

to water molecules. This competition between H_2O molecules and PF_6^- ions was confirmed experimentally: the formation of a complex $UO_2PF_6^+$ was evidenced by TRES but could not be observed by the EXAFS technique, which requires higher uranium concentrations and, thus, higher PF_6^- concentrations (higher than could be possibly made). TRES experiments also showed that PF_6^- dissociation leads to the formation of F^-, the strongest fluorinated ligand to uranyl, which interferes in the complexation process. This means that in $BumimPF_6$, or to a less extent in $BumimBF_4$, the fluoride anions formed by dissociation of PF_6^- and BF_4^- could largely interfere in the complexation processes of uranyl. This dissociation being related to the presence of water in the RTIL, it points out once again the major influence that residual water in RTILs could possibly have.

Calculations show an evolution in U−F bond lengths as a function of the ligand strength: shorter for UO_2F^+ and then longer for $UO_2BF_4^+$ and $UO_2PF_6^+$. On the contrary, the discrimination between each complex is not possible by experimental techniques: similar U−F bond length as measured by EXAFS and similar emission spectra as detected by TRES. Nevertheless, the presence of fluorinated ligands in the uranyl coordination sphere could be clearly evidenced by experimental techniques (longer lifetimes by TRES and a FT splitting in the equatorial shell into shorter distance for U−F by EXAFS).

Acknowledgment. The financial support of the "Groupement de Recherches" PRACTIS/PARIS and grants of computing time from the Norwegian High Performance Computing Consortium (NOTUR) are gratefully acknowledged. We thank K. Lützenkirchen and V. Vallet for fruitful discussions.

IC0490324